modified facility where it appears that the first shock is fully reflected. These observations imply that the cycle first assumed for the original expansion tube—unreflected first shock—should be modified to include reflection of the first shock.

Test times predicted for the modified facility were shorter than observed times. An explanation of this result is that computed test time is very sensitive to velocity in the test section. For example, if a $U_{s_{10}}$ of 5000 m/sec is increased by only 2.5% (within experimental accuracy), the estimated test time is doubled.[4]

## Conclusions

Specific conclusions based on this work are: 1) A high percentage of useful test runs was found in the modified expansion tube using the new nozzle plate (Table 2); 2) The computation model chosen for the modified expansion tube is satisfactory for the range considered here; and 3) It may be inappropriate to assume that the first shock is not reflected from the mylar second diaphragm as had been done in the work on the original expansion tube.

An overview of tests made in our expansion tube leads to the following general remarks: 1) A post-run inspection of diaphragms showed that they opened more cleanly with no measurable loss of diaphragm material more often for the new nozzle plate than for the first nozzle plate; and pitot pressure and density (streak interferometry) measurements showed that the percentage of useful tests was higher for these tests (Table 2) than for tests in either the original expansion tube or the modified tube with the first nozzle plate; 2) Velocity, density, pressure, and testing time measured in the modified expansion tube are comparable to those measured in the original expansion tube; 3) Dissociation computed in the modified expansion tube (full reflection of first shock) is much lower than in similar flow facilities at the same velocity; e.g., shock tunnels; but it can become a factor at flow velocities above ~5500 m/sec[5]; and 4) Radiation measurements[7] and measured relaxation times in Argon[8] indicate that the total impurity level in the modified expansion tube (a few hundred parts per million) is somewhat lower than in the original expansion tube.

## References


[1]Spurk, J.H., Gion, E.J., and Sturek, W.B., "Investigations of Flow Properties in an Expansion Tube," AIAA Paper 68-371, San Francisco, Calif., 1968. Also BRL Rept. 1404, June 1968, AD 673109, U.S. Army Ballistic Research Lab., Aberdeen Proving Ground, Md.

[2]Spurk, J.H., Gion, E.J., and Sturek, W.B., "Modified Expansion Tube," *AIAA Journal*, Vol. 7, Feb. 1969, pp. 345-346.

[3]Spurk, J. H. and Bartos, J.M., "Interferometric Measurement of the Nonequilibrium Flow Field Around a Cone," *Physics of Fluids*, Vol. 9, July 1966, pp. 1278-1285.

[4]Gerber, N., and Bartos, J.M., "Operation Cycle of Expansion Tube with Nozzle Plate," BRL Memo. Rept. 1982, June 1969, AD 689540, U.S. Army Ballistic Research Lab., Aberdeen Proving Ground, Md.

[5]Oertel, F. H., Gerber, N., and Bartos, J.M., "The Modified Expansion Tube: Theory and Experiment," BRL Rept. 1741, Sept. 1974, AD A001551, U. S. Army Ballistic Research Lab., Aberdeen Proving Ground, Md.

[6]Spurk, J. H., "Design, Operation and Preliminary Results of the BRL Expansion Tube," BRL Rept. 1304, Oct. 1963, AD 630065, U. S. Army Ballistic Research Lab., Aberdeen Proving Ground, Md.; also, *Proceedings of the Fourth Hypervelocity Techniques Symposium*, Arnold Air Force Station, Nov. 1965, pp. 111-144.

[7]Spurk, J. H. and Gion, E. J., "Impurity Concentration in the Expansion Tube," *AIAA Journal*, Vol. 7, Feb. 1969, pp. 346-348.

[8]Oertel, F. H., "Measurement of Electron Concentrations in an Axisymmetric Nonequilibrium Shock Layer," BRL Rept. 1594, June 1972, AD 355679, U. S. Army Ballistic Research Lab., Aberdeen Proving Ground, Md.


# Calculation of Transition Matrices


C. von Kerczek*
*University of Maryland, College Park, Md.*

and

S. H. Davis†
*The Johns Hopkins University, Baltimore, Md.*


## I. Introduction

SYSTEMS of linear ordinary differential equations with periodic coefficients arise in the study of the stability of helicopter rotor blade flapping motions,[1-3] the instability of columns under periodic loading,[4] the hydrodynamic stability of periodic laminar flows,[5] and, in general, the stability of systems under parametric excitation.

Such problems reduce to the solution of a system of differential equations such as

$$\dot{y} = A(t)y \tag{1}$$

where $y$ is an $N$-component vector, and $A(t)$ is an $N\times N$ matrix with coefficients having period $T$. The solutions are characterized in the Floquet Theorem[6]; every fundamental matrix solution $\Phi(t)$ of Eq. (1) has the form

$$\Phi(t) = P(t)e^{Ct} \tag{2}$$

where $P(t)$ is an $N\times N$ matrix of period $T$, and $C$ is an $N\times N$ constant matrix. Thus the stability or instability of the null solution of Eq. (1) is determined by the real parts of the eigenvalues $\{\lambda_i\}$ of $C$. The fundamental matrix $\Phi(t)$ that satisfies $\Phi(0) = I$, the identity matrix, is called the *transition matrix*. Using the fact that $P(t)$ is $T$-periodic, one has

$$\Phi(T) = e^{CT} \tag{3}$$

The eigenvalues of $C$ are obtained from the eigenvalues $\{\mu_i\}$ of $\Phi(T)$ by the relation

$$\lambda_i = \ell n\ \mu_i, i = 1,2,\ldots,N \tag{4}$$

The imaginary part of Eq. (4) is defined mod$[2\pi n/T]$. The transition matrix must be obtained by integrating system (1) for the $N$ initial conditions $y_j{}^{(i)}(0) = \delta_{ij}$ where $y_j{}^{(i)}$ is the $j$th component of the $i$th column of $\Phi$.

We first note that any convenient library subroutine that integrates ordinary differential equations can normally be used to obtain the matrix $\Phi(t)$. However, since such subroutines are usually written for the solution of *vector* equations, one should formulate the calculation procedure for the matrix $\Phi$ as one for the calculation of the $N^2$ component vector $(\Phi_{11},\ldots\Phi_{1N},\Phi_{21}\ldots,\Phi_{NN})$. Thus integration to obtain $\Phi(t)$ is accomplished in one sweep (instead of $N$ separate integrations of Eq. (1)) and many evaluations of $A(t)$ are saved.

In most applications where systems such as Eq. (1) arise, a parameter space must be searched for boundaries that separate stable from unstable regions. The transition matrix


Received February 26, 1975; revision received April 14, 1975. This work was partially supported by NSF Applied Mathematics Program, Grant number GP-39933X.

Index category: Structural Stability Analysis.



*Assistant Professor, Mechanical Engineering Department; presently at David Taylor Naval Ship Research and Development Center, Bethesda, Md.

†Professor, Department of Mechanics and Materials Science.

must be computed many times so that a very efficient numerical integration program is desirable. Our main purpose in this Note is to present more efficient and *very easily programed* ways of obtaining the transition matrix. The key feature is the solving for the transition matrix directly from the matrix equation

$$\dot{\Phi} = A\Phi \tag{5}$$

rather than from Eq. (1). This involves matrix multiplications when evaluating the right side of Eq. (5) at each step of the integration instead of the matrix-vector multiplications involved when solving for a vector solution. Matrix multiplications do require $0(N^3)$ operations. However, the solution of the $N \times N$ algebriac matrix system

$$DX = B \tag{6}$$

requires only $0(4N^3/3)$ operations if Gaussian elimination (the $LU$ decomposition of $D$ and back substitution[7]) is used. Thus when numerically integrating Eq. (5), one can use *implicit* integration methods, which require the solution of algebraic systems such as Eq. (6) at each step, for a computational cost which is hardly greater than a single evaluation of the right-hand side of Eq. (5). In particular, single step implicit higher derivative methods give high accuracy and absolute stability and so are advantageous in minimizing the execution time for a *given accuracy*.

To illustrate this point, we compare 3 numerical integration methods in the calculation of a transition matrix. One of these is the fourth-order Runge-Kutta-classic method, which is in very wide use because of its simplicity.[8] Predictor-corrector methods based on multistep formulas of Adams type[8] are also used widely. Since we can use implicit methods economically, one of the methods we have chosen for comparison is the fourth-order Adams-Moulton implicit multistep method, the corrector of a widely used predictor-corrector method.[8] Finally, we have considered a little-used method which involves higher derivatives of the differential equation, and we show that it is the most suitable for calculating transition matrices.

## II. Numerical Integration

The numerical integration methods are applied directly to the matrix form Eq. (5) of the system. The form of the fourth order Runge-Kutta classic method may be found in Ref. 8. It is applied in the usual way to Eq. (5).

The fourth-order Adams-Moulton method[8] applied to Eq. (5) is

$$[I - (9h/24)A_{n+1}]\Phi_{n+1} = \Phi_n + (h/24)[19\dot{\Phi}_n - 5\dot{\Phi}_{n-1} + \dot{\Phi}_{n-2}] \tag{7}$$

where the subscript $n$ refers to the step $t = t_n = nh$. At each step the linear algebraic system, Eq. (7), is solved using Gaussian elimination. If the previous matrices $\Phi_{n-1}$ and $\ddot{\Phi}_{n-2}$ are saved, then at each step one need only compute the matrix product to obtain $\dot{\Phi}_n$ and hence the solution of Eq. (7). The total number of operations per step is thus $0(7N^3/3)$. This is very little more than using the predictor-corrector method based on this formula and has the advantages of greatly enhanced numerical stability and higher accuracy. The *implicit* formula, Eq. (7), has a real numerical stability range which is slightly greater than fourth-order Runge-Kutta method.[8]

The following integration method uses the second derivative of $\Phi$ and is of fourth-order[8]:

$$\Phi_{n+1} = \Phi_n + (h/2)\,[\dot{\Phi}_n + \dot{\Phi}_{n+1}] + (h^2/12)\,[\ddot{\Phi}_n - \ddot{\Phi}_{n+1}]$$

When applied to Eq. (5), the method takes the form

$$[I - (h/2)A_{n+1} + (h^2/12)B_{n+1}]\Phi_{n+1} = [I + (h/2)A_n + (h^2/12)B_n]\Phi_n \tag{8}$$

where

$$\ddot{\Phi} = [\dot{A} + A^2]\Phi \equiv B\Phi \tag{9}$$

Equation (8) is solved at each step in the same way as Eq. (7). At each step the matrix product on the right hand side of Eq. (8), the matrix product necessary for the computation of the matrix $B$ defined in Eq. (9), and the solution of the system of equations require $0[10/N^3/3]$ operations.

The fourth-order Runge-Kutta method requires 4 evaluations of the right-hand side of Eq. (5) per step and hence requires $0(4N^3)$ operations. The main advantages of using Runge-Kutta methods are that they are single step and thus easily programed and have fairly good numerical stability intervals (as compared with predictor-corrector methods). However, the second advantage is nullified when using the fourth-order Adams-Moulton method in implicit form since its stability interval is slightly larger than a fourth-order Runge-Kutta.[8] Better yet, the second derivative method, Eq. (8), is also single step and absolutely stable, and its truncation error is $(1/720)h^5\Phi^V(\xi)$, where $\Phi^V(\xi)$ is the fifth derivative of one component of $\Phi$ and $\xi \in [t_n, t_{n+1}]$. This is smaller (by a factor of almost 20) than the truncation error of the fourth-order Adams-Moulton corrector, Eq. (7): $(19/720)\,h^5\,\Phi^V(\xi)$. One cannot obtain such an explicit truncation error estimate for Runge-Kutta formulas, but previous experience indicates that the accuracy of the fourth-order Runge-Kutta classic is slightly better than the Adams-Moulton method, Eq. (7). Thus one might expect considerably greater accuracy from method Eq. (8), than from the Runge-Kutta or Adams-Moulton method, Eq. (7). The Gaussian elimination and back substitution required in Eqs. (7) and (8) are carried out using the very short and reliable programs of Moler.[9]

## III. An Example

The following test case results from the linear stability theory of a periodic flow examined in Ref. 5.

$$\dot{\Phi} = (P + i\,C\cos t + i\,S\sin t)\Phi \tag{10}$$

The matrices $P$, $C$, and $S$ are real, constant $5 \times 5$ matrics and are given in the Appendix, $i = (-1)^{1/2}$. One can show [5]‡ that

$$\Phi(2\pi) = \Phi^*(\pi)\Phi(\pi) \tag{11}$$

where $\Phi^*$ is the complex conjugate of $\Phi$. Hence, one need only obtain $\Phi(\pi)$. It is also easy to show that the sum of the Floquet exponents, the eigenvalues $\{\lambda_i\}$, are related to $P$ as follows:

$$S = \sum_{i=1}^{5} \lambda_i = \text{trace } P \tag{12}$$

Equations (7) and (8) and the fourth-order Runge-Kutta-classic (denoted by R-K-C) were programed. In Eq. (7), the two extra starting values at $n = 1$ and 2 are obtained by first integrating for two steps using the fourth-order Runge-Kutta method. Comparison of the execution time required to obtain the matrix $\Phi(\pi)$ are made in Table 1. The comparison is based on the accuracy of the value of $\lambda_1$, the Floquet ex-

‡In Ref. 5, the statement $F(t) = F^*(t-\pi)$ on p. 763 should read $F(t) = F^*(t-\pi)C$, where $C$ is a constant matrix.

**Table 1 Results**

| Method | $M$ | $\lambda_1$ | % Error | $S$ | Time (sec) |
|---|---|---|---|---|---|
| R-K-C | 64 | −0.09204 | .... | −8.4235 | 1.82 |
| (7) | 64 | 1.804 | .... | −4.7402 | 1.66 |
| (8) | 64 | −0.1865 | .... | −7.0283 | 2.21 |
| R-K-C | 128 | −0.09447 | 57 | −7.1102 | 3.68 |
| (7) | 128 | 0.03668 | .... | −6.9453 | 3.31 |
| (8) | 128 | −0.06429 | 6.7 | −7.0667 | 4.38 |
| R-K-C | 192 | −0.06749 | 14 | −7.0742 | 5.51 |
| (7) | 192 | −0.03927 | 35 | −7.0580 | 4.96 |
| (8) | 192 | −0.06156 | 2.2 | −7.0693 | 6.61 |
| R-K-C | 256 | −0.06251 | 3.8 | −7.0707 | 7.36 |
| (7) | 256 | −0.05333 | 11 | −7.0681 | 6.58 |
| (8) | 256 | −0.06065 | 0.71 | −7.0698 | 8.74 |
| R-K-C | 384 | −0.06066 | 0.75 | −7.0700 | 11.06 |
| (7) | 384 | −0.05883 | 2.3 | −7.0700 | 9.86 |
| (8) | 384 | −0.06039 | 0.28 | −7.0700 | 13.2 |
| R-K-C | 512 | −0.06036 | 0.23 | −7.0700 | 14.85 |
| (7) | 512 | −0.05978 | 0.73 | −7.0701 | 13.16 |
| (8) | 512 | −0.06033 | 0.18 | −7.0700 | 17.50 |

ponent with largest real part, and $S$. Note that all $\{\lambda_i\}$ are real or conjugate pairs because of the property, Eq. (12). (All $\lambda_i$ are found to be real.)

In Table 1, $M$ denotes the number of equal integration steps that divide the interval $[0,\pi]$. The percent error of $\lambda_1$ is measured relative to the value $\lambda_1 = -0.06022$. This value is obtained using method (8) with $M=896$ and $M=1024$ integration steps. It is presumed to be exact to the number of figures shown. The exact value of $S$ is $-7.07$.

The main results to note in Table 1 are that Eq. (8) is by far the most accurate for a given $M$ and that it requires the most computer time, about 0.034 sec/step vs about 0.026 and 0.029 sec/step for Eq. (7) and R-K-C, respectively. Although Eq. (8) requires theoretically only 0 ($10N^3/3$) operations per step vs $0(4N^3)$ for R-K-C, it is slower on a per step basis because the Gaussian elimination program does partial pivoting and has a relatively high overhead cost. For large $N$, the $0(10\ N^3/3)$ operation count would dominate the time requirement.

The calculation of the eigenvalues of $\Phi(2\pi)$ is carried out by using FORTRAN IV versions of the Algol programs COMHES and LRCOM of Wilkinson and Martin.[10] the machine used is a CDC 6400.

## IV. Conclusions

It can be seen from Table 1 that although Eq. (8) requires the most computer time for a *given number of steps*, its very high accuracy and absolute stability give an *equivalent accuracy*, say to within 1%, in only 4/5 the execution time of the Runge-Kutta and 2/3 of the Adams-Moulton method. Since in most cases $N$ is not small, and the system may be stiff or nearly so,¶ it is advantageous to have an absolute stable numerical integration method. Furthermore, the ease of implementation of Eq. (8), which requires no special starting procedure, makes it the best choice to use when results are to be obtained in a minimum of the investigator's time. For very large systems and systems where $B(t)$ is not easily evaluated, Eq. (7) might be superior, especially if numerical instability is not a problem (i.e., for nonstiff equations). Then implicit Adams-Moulton methods of higher than fourth order can safely be used in exactly the same way as Eq. (7).

¶Because such systems often arise from approximations of partial differential equations which have unbounded sets of eigenvalues.

## Appendix: Matrices $P$, $C$, and $S$

$$P=\begin{bmatrix} -0.320 & 0.000 & -0.380 & 0.000 & -0.900 \\ 0.000 & -0.710 & 0.000 & -0.470 & 0.000 \\ -0.006 & 0.000 & -1.28 & 0.000 & -0.620 \\ 0.000 & -0.040 & 0.000 & -1.950 & 0.000 \\ -0.002 & 0.000 & -0.100 & 0.000 & -2.810 \end{bmatrix}$$

$$C=\begin{bmatrix} 3.43 & 10.7 & 19.5 & 24.9 & 23.9 \\ 5.07 & 8.11 & 11.6 & 16.9 & 20.4 \\ 3.59 & 6.41 & 8.80 & 12.0 & 16.3 \\ 1.50 & 3.63 & 5.25 & 6.79 & 9.41 \\ 0.330 & 1.72 & 3.81 & 5.35 & 6.75 \end{bmatrix}$$

$$S=\begin{bmatrix} 7.82 & 13.0 & 13.1 & 7.04 & -0.480 \\ 3.14 & 6.16 & 9.34 & 9.17 & 3.51 \\ -0.040 & 2.42 & 5.69 & 8.22 & 7.34 \\ -1.24 & -0.530 & 2.27 & 5.25 & 6.87 \\ -0.890 & -1.19 & 0.160 & 2.87 & 5.33 \end{bmatrix}$$

## References

[1] Friedmann, P. and Tong, P., "Aeroelastic Stability of Periodic Systems With Application to Rotor Blade Flutter," *AIAA Journal*, Vol. 12, Nov. 1974, pp. 1559-1565.

[2] Horvay, G. and Yuan, S. W., "Stability of Rotor Blate Flapping Motion when the Hinges are Tilted. Generalization of the 'Rectangular Ripple' Method of solution," *Journal of the Aeronautical Sciences*, Vol. 14, Oct. 1947, pp. 583-593.

[3] Peters, D. A. and Hohenemser, K. H., "Application of the Floquet Transition Matrix to Problems of Lifting Rotor Stability," *Journal of American Helicopter Society*, Vol. 16, No. 2, 1971, pp. 2-9.

[4] Bolotin, V. V., *The Dynamic Stability of Elastic Systems*, Holden-Day, San Francisco, Calif., 1964, pp. 281-433.

[5] von Kerczek, C. and Davis, S. H., "Linear Stability Theory of Oscillatory Stokes Layers," *Journal of Fluid Mechanics*, Vol. 62, No. 4, 1974, pp. 753-773.

[6]Coddington, D. A., and Levinson, N., *Theory of Ordinary Differential Equations*, McGraw-Hill, New York, 1955, p. 78.
[7]Isaacson, E. and Keller, H. B., "Analysis of Numerical Methods," Wiley, New York, 1966, p. 29.
[8]Lapidus, L. and Seinfeld, J. H., *Numerical Solution of Ordinary Differential Equations* , Academic Press, New York, 1971, pp. 49, 180, 29.
[9]Moler, C. B., "Algorithm 423: Linear Equation Solver [F4]," *Communications of the ACM*, Vol. 15, No. 4, 1972, p. 274.
[10]Wilkinson, J. H., and Reinsch, C., *Linear Algebra*, Springer, Berlin, 1971, p. 296.

# Static Pressure Rise in Acoustically Driven Cavities

Leslie S.G. Kovasznay* and Ho, Chih-ming†
*The Johns Hopkins University, Baltimore, Md.*

PARALLEL uniform flow over a solid wall creates a boundary layer that is laminar or turbulent according to the flow parameters (Reynolds number, roughness of the wall, disturbance level in the flow), and its thickness increases monotonically from the leading edge. If the continuity of the wall is interrupted by a cavity (either a rectangular cutout or a cylindrical well) the boundary layer may separate locally upstream of the cavity and reattach downstream of it. Inside the cavity an unsteady internal flow pattern may develop[1,2] causing pressure fluctuations and intensive acoustic radiation from the orifice of the cavity.[3]

In the present study, it was experimentally established that the presence of an acoustic oscillation inside the cavity strongly alters the mean pressure level there, namely, it causes a steady (d.c.) pressure monotonically increasing with the sound amplitude within the cavity. In order to establish the amplitude and frequency dependence of this pressure rise, the cavity was "driven" by a loudspeaker so that pressure fluctuations of known frequency and amplitude were imposed.

## Equipment

The experimental configuration consisted of a flat plate 90 cm long, 30 cm wide, and 0.75 cm thick with beveled leading edge placed into the 30×30 cm open working section of an open return wind tunnel (Fig. 1). The plate was equipped with a cylindrical well of $D=2.54$ cm diameter and of $H=11.35$ cm depth located 11.5 cm downstream from the leading edge. The lower end of the cavity was attached to a low-frequency loudspeaker (woofer) and the whole assembly was hermitically sealed in a flexible plastic bag. This arrangement permitted oscillations and prevented a steady flow through the cavity, so that a steady pressure level could be built up in the cavity. When a static pressure rise developed in the cavity, the plastic bag became fully inflated. The freestream velocity was $U_\infty = 3730$ cm/sec. Measurements were taken under three conditions. The nominal boundary-layer thickness $\delta$ (defined as $y=\delta$ where $\bar{U}(y)=0.99\ U_\infty$) and the displacement thickness

$$\delta_* = \int_0^\infty (1-\bar{U}/U_\infty)\,dy$$

Received February 28, 1975; revision received May 19, 1975. Work performed under sponsorships of USAFOSR and USAROD. Assistance of George Sauter, Stuart Dickinson, and Michael Godack is acknowledged.
Index categories: Nonsteady Aerodynamics; Jets, Wakes, and Viscid-Inviscid Flow Interactions.
*Professor of Aeronautics, Department of Mechanics and Materials Science. Member AIAA.
†Associate Research Scientist, Department of Mechanics and Materials Science. Member AIAA.

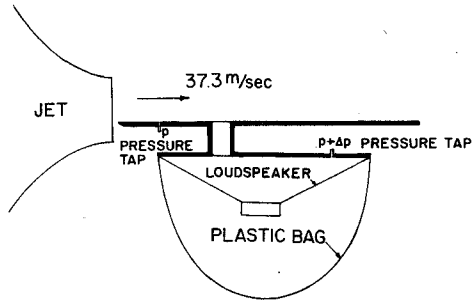


**Fig. 1 Experimental facility.**

**Table 1 Boundary-layer thickness**

| Roughness (cm) | $\delta$ (cm) | $\delta_*$ (cm) |
|---|---|---|
| No roughness | 0.45 | 0.08 |
| Step 0.127 | 1.50 | 0.22 |
| Step 0.208 | 1.60 | 0.31 |

were determined for all three cases. The first condition was with no roughness on the plate. The second and third conditions were made by an artificially thickened boundary layer. Two different roughness elements were used: one was produced by a thin step, and the other produced by a thick step attached to the plate near the leading edge (Table 1).

The static pressure in the cavity was measured by using an inclined tube liquid manometer. The velocity amplitude of the imposed oscillations was measured in still air ($U_\infty = 0$) by placing a hot-wire anemometer in the plane of the flat plate at the center of the orifice. From the measured velocity amplitude $\hat{V}$, the displacement amplitude $\hat{A}=\hat{V}/2\pi f$ was calculated to characterize the magnitude of the oscillations.

It was assumed that the amplitude of the oscillation in the cavity with flow was essentially the same as with no flow. In other words, it was assumed that the change in the acoustic impedance of the cavity orifice due to the mean flow was considered negligible.

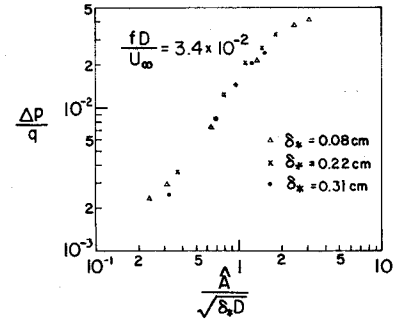


**Fig. 2 Data scaling for three different boundary layers,**

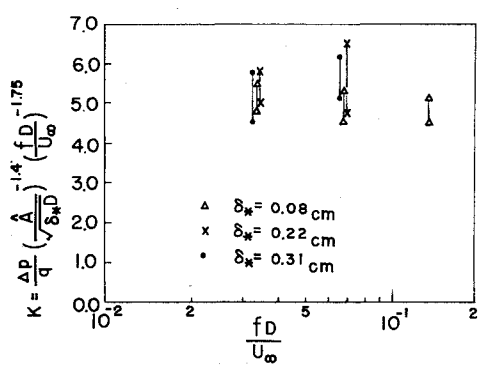


**Fig. 3 Determination of constant K.**